

Automatic Detection and Classification Of Melanoma Skin Cancer through Deep Learning Techniques

¹Sri Geetha M, ²Dr. A. Grace Selvarani, ³Dr. Ravi Kumar, ⁴Dr. Sheshang Degadwala, ⁵Ravi Kishore Veluri

¹Assistant Professor, Department of Computer Science & Engineering, Sri Ramakrishna Engineering College, Coimbatore, srima235@gmail.com (first author)

²Professor, Department of Computer Science & Engineering, Sri Ramakrishna Engineering College, Coimbatore, graceselvarania@gmail.com

³Associate Professor, Department of Electronics and Communication Engineering, Jaypee University of Engineering and Technology, Guna, ravi.kumar6@gmail.com.

⁴Associate Professor, Department of Computer Science & Engineering, Sigma Institute of Engineering, Vadodara, sheshang13@gmail.com

⁵Associate Professor, Department of Computer Science & Engineering, Aditya Engineering College (A), Surampalem, ravikishorev1985@gmail.com

Abstract

In terms of mortality, skin cancer is one among the deadliest forms of cancer. A consistent automated method for skin lesion recognition is required for initial identification. This paper proposes an automated method for classifying skin cancers. The goal is to create a model that uses Deep Learning algorithms to diagnose skin cancer and classify it into several types. Various computer-aided solutions for the correct identification of melanoma cancer have been offered. A reliable CAD system, however, for exact melanoma identification is extremely difficult to develop. Classic learning machines or deep learning approaches are used in existing systems. We suggest the use of an intelligent Region of Interest (ROI) system based on transference learning to recognize and distinguish between melanoma and other cancers. The ROIs are obtained using an enhanced k-mean method. The suggested ROI-based transference learning strategy shows good performance than the previous classification systems that utilize entire images.

Keywords: Deep Learning, classification, Skin cancer, melanoma.

1 Introduction

Melanoma is a malignant condition that assaults the skin, in the cells which manufacture melanin as the shade of UV skin insurance, in which telephones appear to produce melanocytes. This is an abnormal opening to daylight, most of the main drivers of malignant skin melanoma. Bright daylight might affect the skin's well-being. Bright light on destructive skin cells with energy, especially color the skin to be particular melanin. Most incidences of melanoma are caused by daytime openness. Many moles or patches on the skin and pale cleansing are certain components that can promote melanoma. Cancer melanoma is a sickness that occurred on the globe as often as possible in the 19th century. The least is the case. There are approximately 3300 incidences of new melanoma in 2014. Although this type of malignancy is as low, If not the position from the start(Alcón, J.F, et al.,2009), it may be fatal. Dermoscopy is the famous method of melanoma differentiation. The dermoscopic examination is

conducted as a tool employed by an expert dermatologist who knows whether a melanoma from a common mole is suspected or not. It is usually uttered humbly. Be that as it may, the analysis relies upon the experience and expertise of a doctor (Andre Esteva, et al., 2017). As of late, there have been numerous examinations that have utilized different to recognize melanoma malignant growth like For example the morphology research (Almansour, et al.,2016), PC-supported strategy (BilqisAmaliah, et al. ,2010) and the implementation of a second cell phone application, using programmed ABCD rules[Irawan, et al. (2018)] or new strategies from the store application to the play store(Salem, et al. ,2017). 132,000 cases of malignant skin growth are internationally studied according to the World Health Organisation. In 2012, 232,000 people experienced melanoma, and 55,000 people passed by (Farooq, et al.,2016).In Australia and New Zealand, 71 cases per 100,000 people were the most notable rate of melanoma in the world, compared to the multiple in Canada, the UK, and the United States(Rogers, et al. ,2015). More than 8,500 people are reported to have been diagnosed with skin problems in the US continually (Kong, et al. ,2018). In 2016, the USC will assess about 76,380 (46,870 males, 29,510 women) and about 10,130 melanoma crossings (6,750 men, 3,380 ladies). The melanoma risk is approximately 2.4 percent. white(one out of 40); in blacks 0,1% (1 out of 1,000); and in Hispanics 0,5% (one out of 200)[7]. Therefore, it is vital to find early melanoma.

2 Literature survey

Some of the most common skin cancer detection procedures are discussed in this segment.

It was postulated by Ganster et al. that skin images may be used to identify severe melanoma. From the start, for the division reason, fundamental calculation together with a combination procedure is utilized. KNN is then divided into three kinds of benign, dysplastic, and hazardous skin sore melanoma.

Alcon et al.,(2009) proposed a framework that chips the traditional graphics and conveys ABCD's (E)-accuracy for a certain chemical. In order to increase the accuracy, different measures such as age, number of lesions, sunburns, and so on that reflect the overall danger must also be taken into account in conjunction. Image categorization results are combined with setting information in this fashion; (for example, skin type, age, sex, and influenced body part).

Vyanza,(2018) developed an imaging frame for mobile melanoma diagnostics, and all of it is running on mobile phones. It presents a number of hurdles, as the mobile phone's ability to conduct such operations is dependent on calculations and memory needs, and the photographs are taken in a less-than-optimal environment. Skin photos were cleaned up by removing highlights of shading variation and border irregularity. It's a matter of choosing a modest number of good features for the lightweight framework.

It has been hypothesized that the non-dermoscopic computerized photographs of skin can be used to determine the site of a melanoma skin cancer. Injury tone, sore surface, and visual diagnostic aspects of the patients are addressed in this framework. The shading and surface characteristics shall of course be distinguished from the computerized images, though the inspector determines the presence and non-attention of a set of visual qualities. Using the democratic technique from three sources, the latest categorization choice is taken for experiments.

Yuexiang et al.,(2018) proposed a system for autonomous diagnostics to help identify the malignant growth of melanoma skin in images captured by the camera. The division is finished in the HSV shading room by applying K-implies and numerous activities are followed. SVM classifier classifies the picture as melanoma or favorable based on parameters such as imbalance, line, and shade.

Shen et al., (2018) presented a mobile-enabled method for melanoma detection that would be available to the general public. In order to group the data, the SVM classifier was applied. There is still a lot of progress in the field of melanoma skin malignant development is an extent of progress and need to foster a framework that can effectively analyze melanoma.

3 Research methodology

Pictorial outline of skin malignant growth recognition is shown below Figure 1. The first picture below shows the cancer of the skin. Some hair and air bubbles in this photo detract from the accuracy of the composition. In the next process, the hair is removed.

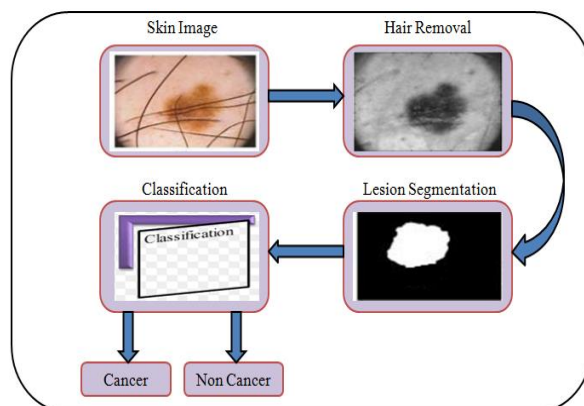


Fig 1: Overview of skin cancer screening

After hair removal, the image is split to remove the painful area. Highlight extraction, followed by grouping, is used to acquire unique highlights after division. Figure 1 shows this load of steps.

3.1 System Flow Diagram

Four phases are provided for PC-based recognition of skin malignancy: image Pre preparation, picture division, extraction of features, and groups. The picture of the skin altered by melanoma is shown in the context. To enhance the quality of the photograph, this image has been pre-processed in advance. Using image segmentation techniques, the lesion component is separated from the skin after pre-preparation. This is followed by a feature extraction process, which removes the particular highlights. In order to classify the image as benign sore and melanoma skin condition, grouping is performed after feature extraction. Figure 2 shows the system flow diagram.

3.2. Image Pre-processing

The progress underpinning the image handling is pre-preparation, as indicated in Figure 2. The skin picture is a part of the framework. Unwanted elements such as hair and air can be found in this image. As a result, segmentation and consolidation results are weakened. The image is changed to a dark tone in this framework. For eliminating hairs Gaussian channel was utilized (Codella et al.,2017).

3.3. Image Segmentation

The Revenue District (ROI) is divided from the picture called the photograph. This is Figure 2's second stage. The skin image also includes the sound component as the lesion. Taking both parts for additional handling may give less precise grouping results. Just the sore part is needed for picture examination with the goal that division is performed. Segmentation takes the Otsu threshold method(Halpern,2019), which changes over a double image. Following the Otsu thresholding, the yield image is irregular. For the smoothing of the edges, the morphological filter is used(Stoecker,2015).

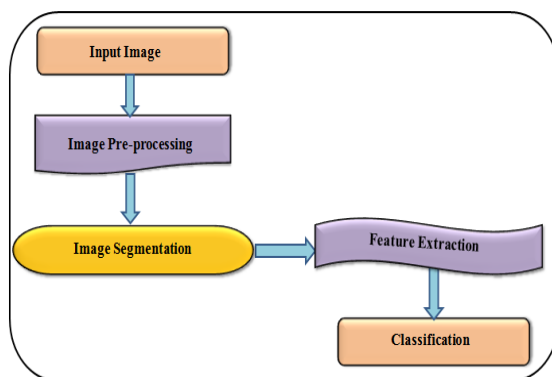


Fig 2: Flow chart of the system

3.4. Feature Extraction

The most outstanding extraction is the technology for the image's distinctive characteristics. These highlights address the information image attributes. This is a crucial step forward. The shading diversity of the melanoma skin images is uniform in tone. Another contrast is the circular form of the benign lesion in which melanoma has an unpredictable form. In this context, the tone of the edge, the region, and the incoherent texture is removed from the skin image along these lines (Reda Kasmi, et al.,2016).

3.5. Classification

Information characterization is perhaps the most dynamic human undertakings (Rubin, et al. ,2006). The melanoma harm caused by generous sore is classified in this progression. Defined as a major advance in terms of the choice of classifier A kindhearted sore SVM classifier is used to classify melanoma. Al

support vector machines are supervised learning models that are commonly used for categorization in the field of artificial intelligence (AI) (Ratnasari, et al., 2018). Selection limits are characterized by the hyperplane. To recognize classes, SVM hyperplane separates them. SVM uses direct capacity and outspread premise work to categorize the information as dangerous or benign, respectively.

3.6 Skin Cancer Data Augmentation

A lot of information model prompts influence the distribution of numerous CNN (Mane, et al., 2017). The issue that may happen in the preparation of deficient information is overfitting. As a rule, the training information accessible for



Fig 3: Samples of segmented ROI

due to unequal distribution of classes. When we look at the insufficient information tests for skin cancer, we employ conventional increase approaches, including cutting the early photographs, to widen the image tests. At 270 degrees, flipping the coin, reflection, and revolution on the right side, the left, and from the base side of 270, each image receives 7 more stunning examples.

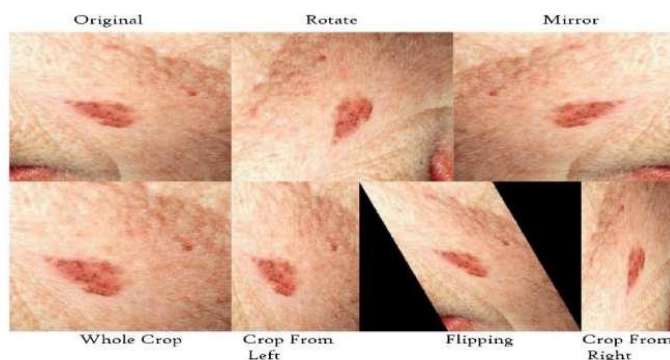


Fig 4: Melanoma sample Images enhanced

3.7 Skin Cancer Diagnosis using Transfer Learning Approach

We have redesigned images as AlexNet prerequisites after the expansion of information checks. Current information does not provide enough examples for the preparation of the new CNN model (Yading

Yuan, 2017). The exchange learning approach is therefore used to address this topic. This pre-trained model is prepared using another authentic dataset in low-level highlights from AlexNet.

a) First Input Layer

All of the scaled amplified data is delivered as a contribution to this layer in this originally input layer of CNN.

b) Convolutional Layers

The most critical layers in all CNNs are concentration layers. The whole work is covered by layers. It performs convolutionary activities on the information and then transmits this reaction to the next required layer. The convolutionary layers enable layers near the input to achieve low levels, deeper concentration, or class highlights

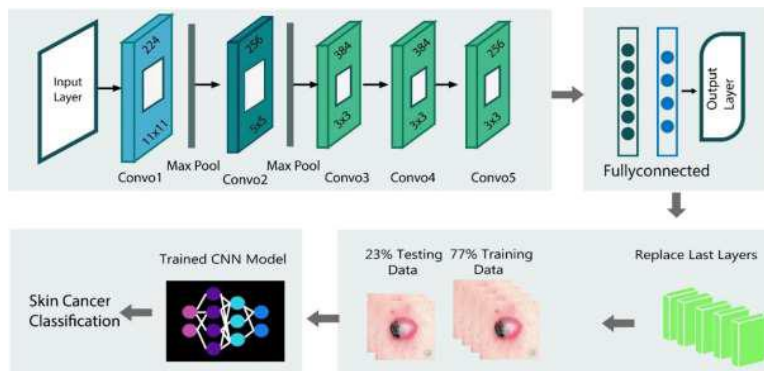


Fig 5: Full Learning Flow Diagram for Transfer

c) Max-Pooling Layers

In the center, there are convolutionary layers that reduce the representation of the pixels and the cost of processing. The pooling layer operates on each pixel of the image to reduce the cost of calculating the next layer. The component map is genuinely a channel. It's like it works. The map size is much larger than the pool size. The group layer is virtually 2x2, a 2-point stride, which decreases the element map by 2 factors in the pooling layer. Our model incorporated the max pooling layer in the intermediate convolutionary layer to provide the highest reward for each article map.

d) Fully Connected Layers

The component map has been deleted from the info images, and the convolution and max-pooling layers have been used to reduce the size of the component map. According to the number of classes with fully linked layers, the end result is the number of classes with fully connected layers. For the

AlexNet construction, images with 227x227x3 measurements and 96 components with a measurement width of 227x227 with a depth of 3 measured in red, green, and blue are filtered by the initial cooling layers. The cooling layer's primary map is passed through the maximum bundling layer to eliminate highlights and send the new element guide to the next cooling layer of 255x5x48 sizes. In addition, by the maximum pooler of 384 sections in the number connected with the third convolution layer, the implications of these second convolution layers are therefore reduced. These are the last three convolutions

The fourth and fifth convolution layers contain a total of 384 256-bit variables. Fully linked layers complete the high-level reasoning within the neural architecture after all the convolutionary layers and pooling levels. The number of neurons in a completely linked layer is 4096. Each neuron interfaces with the neuron in the subsequent layer entirely linked layers. Neurons are associated with all previous layers in the fully connected layers.

e) Replacing Last Layers

Typically the low-level highlights on the underlying layer of the organization are mostly edges, lines, and designs while the explicit element of the class is on the last layer in the organization. Therefore, we are concerned with preparing skin information. Class-explicit highlights were thus provided with new layers, meaning that we substituted SoftMax for the characterization layer, tweaking all loads. The component map of convolution layers is shifted and replaced by class-specific layers. We have used several frontiers, such as the weight learning factor, and Bias learns how to make the connected layers. These training limits control the network's learning pace.

f) Network Training and Testing

Five relocated layers and three new layers for variation exist in this organization. At initially, an insufficient number of tests is performed for the organization in the information test. By expanding and moving the layers, we have overcome the problem. For training and testing data sets, we have employed increased techniques. Only the new layer of malignancies is prepared for precise grouping.



4 Results And Discussion

XiaomiRedmi Note 2 (13 MP), 2-specimen mobile phones, and Samsung Tab S test are included (8 MP). This is a dermoscopic picture knowledge base using a PH2 computerized clinical picture dataset to research and assess the skin using histological determination. There are 40 photographs including 20 beneficent images and 20 melanoma for detailed testing. We examine a photo from each smartphone's printed image.

4.1. Testing with Benign Data




There is a different result in one picture. There was no such result from IMG 0014. A characteristic result is the different pixels and sensors. Table I explains the different outputs

Table I.Different Crop Result

Different crop result	
	
Redmi Note 2	Samsung Tab S
TDS = 4.93	TDS = 4.73

The difference is due to the fact that the Samsung cell phone's shading is more detailed and vibrant. Using only the OmniVision sensor, Samsung claims to be able to identify results from the Xiaomi redmi note 2. The result of the examination camera, Table II, received from analysts from the site of Gsmarena.com[9], is supported.

Table II.Capture Color Different Range

Original Image	Redmi Note 2	Samsung Tab S
		

Diverse reach shading that acquired from both smartphones made distinctive harvest result from every gadget.



4.2. Testing with Melanoma Data

IMG 002 is one of the images that produces the same fake result (fig 6).

Fig 6: Make the same image outcome



Table III. Different crop from fig. 6

	
Redmi Note 2	Samsung Tab S
Result = 3.77	Result = 4.03

The outcome from Table III has given false classification. The reasons for the blunder are because the shading in the figure is excessively faint and hard to catch and prepared with OpenCV as well. The models on both cell phones make different results particularly on the diverse harvest from range tone.

5 Conclusion

Skin disease stays perhaps the most widely recognized and serious type of malignant growth. CAD systems that can extract the most discriminating highlights organically and effectively identify patients are urgently needed. For skin cancer detection, scientists have utilized a variety of methods. This is despite the fact that these strategies require the assistance of a human specialist in order to identify these highlights. Using the AlexNet model, a transfer learning-based productive methodology is proposed to accurately define and recognize skin malignant growth melanoma. Using Region of Interest-based images, the proposed framework removes only discriminatory highlights. DermIS and DermQuest's ROIs and DermIS's unique pictures were used in our studies. As training images, these datasets suffer class awkwardness issues. For this, we combined transfer learning with significant augmentation. As their original and non-developmental concepts approach, we have repositioned the AlexNet model's low-level base layers and examined ROI increases.

References

1. Ahmed Abdelgawad¹ ; Kumar Yelamarthi¹ and Ahmed Khattab², "IoT-Based Health Monitoring System for Active and Assisted Living," Second International Conference from book Smart Objects and Technologies for Social Good, pp.11-20, 2016.
2. Alcón, J.F., et al., Automatic imaging system with decision support for inspection of pigmented skin lesions and melanoma diagnosis. IEEE Journal of selected topics in signal processing, 2009. 3(1): p.14-25.
3. Andre Esteva, Brett Kuprel, Roberto A. Novoa, Justin Ko, Susan M. Swetter, Helen M. Blau, and Sebastian Thrun, "Dermatologist-level classification of skin cancer with deep neural networks", Springer Nature, Vol 542, p-115-127, Feb-2017
4. Almansour, E. and M.A. Jaffar, Classification dermoscopic skin cancer images using color and hybrid texture features. IJCSNS Int J Computer SciNetw Secure, 2016. 16(4): p. 135-9.
5. BilqisAmaliah, ChastineFatichah, and M. RahmatWidyanto, "ABCD Feature Extraction of Image Dermatoscopic Based on morphology Analysis for Melanoma Skin Cancer Diagnosis., "2010.

6. D. F. Azid, B. Irawan and C. Setianingsih, (support vector machine)," inAsia Pacific Conf. Wirel. Mobile, 2018.
7. El-Dahshan, E.-S. A., T. Hosny, and A.-B. M. Salem, "Hybrid intelligent techniques for MRI brain images classification," *Digital Signal Processing*, Vol. 20, No. 2, 433–441, 2018.
8. Farooq, M.A., M.A.M. Azhar, and R.H. Raza. Automatic Lesion Detection System (ALDS) for skin cancer classification using SVM and neural classifiers. in 2016 IEEE 16th International Conference on Bioinformatics and Bioengineering(BIBE). 2016. IEEE.
9. H. Rogers, M. Weinstock, S. Feldman and B. Coldiron, "Incidence Estimate of Nonmelanoma Skin Cancer (Keratinocyte Carcinomas) in the US Population, 2012", *JAMA Dermatology*, vol. 151, no. 10, p. 1081, 2015.
10. Kong, B., et al. Invasive cancer detection utilizing a compressed convolutional neural network and transfer learning. in *International Conference on Medical Image Computing and Computer-Assisted Intervention*. 2018. Springer.
11. M. A. L. M. Boone Email, M. SuppaF, DhaenensM, Miyamoto, "In vivo assessment of optical properties of melanocytic skin lesions and differentiation of melanoma from non-malignant lesions by high-definition optical coherence tomography," *Archives of dermatological Research*, 2016.
12. N. C. F. Codella, Q. Nguyen, S. Pankanti, D. Gutman, B. Helba, A. Halpern, and J. R. Smith, "Deep learning ensembles for melanoma recognition in dermoscopy images," *IBM Journal of Research and development*, vol. 61, no. 4/5, pp. 5:1-5:15, 2017.
13. N. C. Codella, D. Gutman, M. E. Celebi, B. Helba, M. A. Marchetti, S. W. Dusza, A. Kalloo, K. Liopyris, N. Mishra, H. Kittler, et al., "Skinlesion analysis toward melanoma detection: A challenge at the 2017 international symposium on biomedical imaging (ISBI), hosted by the international skin imaging collaboration (ISIC)," in 2018 IEEE 15th International Symposium on Biomedical Imaging (ISBI 2018). IEEE, 2018, pp. 168–172.
14. O. Reiter, A. C. Halpern, S. Puig, and J. Malveyh, "Bcn20000: Dermoscopic lesions in the wild," *arXiv preprint arXiv:1908.02288*, 2019.
15. P. Kharazmi, H. Lui, W. V. Stoecker, and T. Lee, Automatic detection and segmentation of vascular structures in dermoscopy images using a novel vesselness measure based on pixel redness and tubularness, *Proc. SPIE*, vol. 9414, 2015
16. Reda Kasmi, Karim Mokrani, "Classification of malignant melanoma and benign skin lesions: Implementation of automatic ABCD rule," 2016.
17. Rubin, Adam I., Elbert H. Chen, and Désirée Ratner, "Basal-cell carcinoma", *New England Journal of Medicine*, vol. 354, no. 7, pp. 769-771, 2006.
18. R. Ratnasari, B. Irwan and C. Setianingsih, "Traffic sign recognition application using scale-invariant feature transform method and support vector machine based on android," in *Asia Pacific Conf. Wirel. Mobile*, 2018.
19. S. S. Mane, S. V. Shinde, "Different Techniques for Skin Cancer Detection Using Dermoscopy Images", *International Journal of Computer Sciences and Engineering*, Vol. 5, Issue. 12, pp. 165-170, 2017.

20. Taufiq, M.A., et al., m-Skin Doctor: a mobile-enabled system for early melanoma skin cancer detection using support vector machine, in *eHealth360°*. 2017, Springer. p. 468-475.
21. Verkouteren, J. A. C., K. H. R. Ramdas, M. Waukee, and T. Nijsten" Epidemiology of basal cell carcinoma: a scholarly review", *British Journal of Dermatology*, vol. 177, no. 2, pp. 359-372, 2017.
22. V. E. Vyanza, B. Irwan and C. Setianingsih, "Design of smart door system for live face recognition based on image processing using principal component analysis and template matching correlation methods," in *Asia Pacific Conf. Wirel. Mobile*, 2018.
23. Xie, F., et al., Melanoma classification on dermoscopy images using a neural network ensemble model. *IEEE transactions on medical imaging*, 2016. 36(3): p. 849-858.
24. Yuexiang Li, Linlin Shen, "Skin Lesion Analysis towards Melanoma Detection Using Deep Learning Network", *Sensors*, p-1-16, 2018.
25. Y. Li and L. Shen, "Skin lesion analysis towards melanoma detection using deep learning network," *Sensors*, vol. 18, no. 2, pp.556, 2018.
26. Yading Yuan, Ming Chao, Yeh-Chi Lo, "Automatic Skin Lesion Segmentation Using Deep Fully Convolutional Networks with Jaccard Distance", *IEEE Transactions on Medical Imaging*, Vol. 36, Issue 9, Sept. 2017, IEEE 2017.